THE INFLUENCE OF A HOMOGENEOUS EXTERNAL MAGNETIC FIELD AND SINGLE-ION ORTHORHOMBIC ANISOTROPY ON THE STABLE SPIN CONFIGURATIONS IN THE TWO-SUBLATTICE NEEL-TYPE ANTIFERROMAGNET

By W. Prystasz and G. Kozłowski

Institute for Low Temperature and Structure Research, Polish Academy of Sciences, Wrocław*

(Received May 15, 1979)

By minimizing the approximate ground state energy of the two-sublattice Neel-type antiferromagnet with exchange-type and orthorhombic single-ion anisotropy, the stable magnetic phases in an arbitrary directed external magnetic field were studied. It is shown that for certain magnetic fields two kinds of metastable spin configurations can occur which are dependent on the effective single-ion anisotropy with respect to the direction preferred by the exchange interactions. For a sufficiently strong single-ion anisotropy in the easy direction, the possibility for the coexistence of the stable canted-spin and ferromagnetic phases was also found.

1. Introduction

During the last few years the field-induced phase transitions in antiferromagnets were intensively studied both experimentally and theoretically. It was found that the external magnetic field parallel to the easy axis of the antiferromagnet induces the two phase transitions. The first-order transition is between the antiferromagnetic phase (AF) and spin-flop phase (SF). The second-order phase transition is between the spin-flop phase and the paramagnetic phase. Detailed theoretical investigations of these phase transitions can be found [1], where in particular, the temperature dependence of the critical fields is given. This dependence was studied experimentally for $McCl_2 \cdot 4H_2O$ [2] and for $CoCl_2 \cdot 6H_2O$ [3]. The $T^{5/2}$-law [1], which should govern the low temperature dependence of the critical field at the phase transition from SF to P, was not confirmed [2, 3]. It was stated [4] that the transversal exchange anisotropy in $CoCl_2 \cdot 6H_2O$ and single-ion orthorhombic anisotropy in $MnCl_2 \cdot 4H_2O$ is responsible for the deviation from the $T^{5/2}$-law, and therefore the T^2-dependence was proposed.

* Address: Instytut Niskich Temperatur i Badań Strukturalnych PAN, Plac Katedralny 1, 50–329 Wrocław, Poland.

The essential influence of the single-ion anisotropy on the occurrence of phase transitions was found previously [5, 6]. These investigations, which were confined to $T = 0$ K, showed in the presence of the field parallel to the easy axis the fourth phase, namely the canted-spin phase (CS) can occur. This phase separates the phases AF and SF and the phase transitions AF $\leftrightarrow$ CS, CS $\leftrightarrow$ SF and SF $\leftrightarrow$ P were found to be of the second order. Phase diagrams at $T = 0$ K for an antiferromagnet with the single-ion anisotropy in the presence of the external field of an arbitrary direction were determined [7, 8]. The results [7] were based on numerical analysis and the analytical considerations [8] are confined to small anisotropies. However the phase diagram determined [9] is valid within the limits of large single-ion anisotropies (metamagnet) at $T = 0$ K.

2. Determination of the ground state and stability regions

As in [10] we shall consider the antiferromagnet with the orthorhombic single-ion anisotropy and perpendicular exchange anisotropy at $T = 0$ K in the external magnetic field having an arbitrary direction. The Hamiltonian of our system can be represented as:

$$\mathcal{H} = J \sum_{\langle f,g \rangle} (X S_f^x S_g^x + S_f^y S_g^y + Z S_f^z S_g^z) - \mu H_x [\sum_f S_f^x + \sum_g S_g^x]$$
$$- \mu H_z [\sum_f S_f^z + \sum_g S_g^z] - L_x [\sum_f (S_f^x)^2 + \sum_g (S_g^x)^2] - L_z [\sum_f (S_f^z)^2 + \sum_g (S_g^z)^2], \tag{1}$$

where $X = 1 + K_x/J$, $Z = 1 + K_z/J$. The indices $\langle f, g \rangle$ denote the lattice sites of the first and second sublattice, respectively. The summation over $\langle f, g \rangle$ is restricted to the nearest neighbours. $K_x > 0$, $K_z > 0$ are exchange anisotropy constants in the directions x and z. $J > 0$ is the exchange integral between the nearst neighbours of the different sublattices. μ stands for the effective magnetic moment per site. H_x, H_z are the components of a homogeneous, external magnetic field and $L_x > 0$, $L_z > 0$ are the single-ion anisotropy constants.

Applying the formalism introduced in [11, 12], we can determine the approximate ground state of the Hamiltonian (1) by minimizing its mean value in the class of sublattice saturation states. If we assume that in the saturation state the magnetic moment of each sublattice lies in the plane xy, then the reduced mean value of the Hamiltonian (1) can be written in the following way:

$$E = \tfrac{1}{2}(X - Z)\cos 2\beta - \tfrac{1}{2}(X + Z)\cos 2\alpha - a \cos 2\beta \cos 2\alpha - 2 \sin \alpha (h_x \cos \beta + h_z \sin \beta), \tag{2}$$

where S is the maximum spin eigenvalue and

$$h_{x,z} = \mu H_{x,z}/\gamma_0 JS, \quad 2\alpha = \varphi + \theta, \quad 2\beta = \varphi - \theta, \quad 2a = (2S-1)(L_z - L_x)/\gamma_0 JS,$$

and γ_0 denotes the number of the nearest neighbours.

In the absence of the external magnetic field the stable antiferromagnetic configuration is parallel to the x-axis if $X - Z > 2a$.

The stable configurations and the range of their stability are obtained by solving the necessary and sufficient conditions for a minimum with respect to α and β

$$\frac{\partial E}{\partial \alpha} = \frac{\partial E}{\partial \beta} = 0, \quad \Delta = \frac{\partial^2 E}{\partial \alpha^2} \cdot \frac{\partial^2 E}{\partial \beta^2} - \left(\frac{\partial^2 E}{\partial \alpha \partial \beta}\right)^2 \geqslant 0, \quad \frac{\partial^2 E}{\partial \alpha^2} \geqslant 0. \tag{3}$$

The condition $\partial E/\partial \alpha = 0$ leads to

$$\cos \alpha = 0, \tag{4}$$

$$(X+Z+2a \cos 2\beta) \sin \alpha - (h_x \cos \beta + h_z \sin \beta) = 0, \tag{5}$$

whereas $\partial E/\partial \beta = 0$ yields:

$$(Z-X+2a \cos 2\alpha) \sin 2\beta + 2 \sin \alpha (h_x \sin \beta - h_z \cos \beta) = 0. \tag{6}$$

The system of equations described above cannot be solved analytically for an arbitrary directed magnetic field except for certain well known cases, namely, when the field is parallel ($h_z = 0$) or perpendicular to the easy axis. These solutions, their stability ranges

TABLE I

The stable solutions of (4)–(6) in the easy $h_z = 0$ or perpendicular $h_x = 0$ and their stability ranges and energy

$\gamma = \frac{\pi}{2}$	$h_z = 0$		
Phase	stability range	energy	solutions with respect to α and β
AF	$0 \leqslant h_x \leqslant h_1^x$	$-X+a$	$\sin \alpha = 0, \quad \cos \beta = 0$
CS	$h_1^x \leqslant h_x \leqslant h_2^x$	$-X+a-\frac{(h_x-h_1^x)^2}{4a}$	$\sin^2 \alpha = (h_x-h_1^x)\sqrt{\frac{B}{h_1^z}}\Big/4a$ $\cos^2 \beta = (h_x-h_1^x)/4a \cdot \sqrt{\frac{B}{h_1^z}}$
SF	$h_2^x \leqslant h_x \leqslant h_3^x$	$-Z-a-\frac{h_x^2}{h_3^x}$	$\sin \alpha = \frac{h_x}{h_3^x}, \quad \sin \beta = 0$
P	$h_3^x \leqslant h_x$	$X+a-2h_x$	$\sin \alpha = 1, \quad \sin \beta = 0$
$\gamma = 0$	$h_x = 0$		
SF	$0 \leqslant h_z \leqslant h_1^z$	$-X+a-\frac{h_z^2}{h_1^z}$	$\sin \alpha = \frac{h_z}{h_1^z}, \quad \cos \beta = 0$
P	$h_1^z \leqslant h_z$	$-Z-a-2h_z$	$\cos \alpha = 0, \quad \cos \beta = 0$

and the corresponding energies are given in Table I. The critical fields introduced in Table I are the following:

$$h_1^x = [(X-2a)^2-Z^2]^{1/2}, \tag{7}$$

$$h_2^x = (X+Z+2a)\sqrt{\frac{B}{h_1^z}} = h_3^x\sqrt{\frac{B}{h_1^z}}, \tag{8}$$

$$h_3^x = (X+Z+2a), \tag{9}$$

$$h_1^z = (X+Z-2a), \quad B = (X-Z-2a). \tag{10}$$

In spite of the difficulties in finding the analytical solutions of (4)–(6), one can determine the behaviour of spin configurations under the influence of the field of an arbitrary

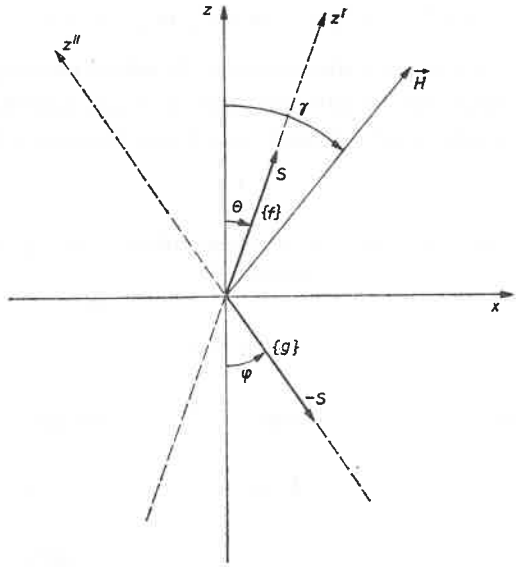

Fig. 1. The assumed coordinate system: angle γ measures the direction of the external magnetic field, the angles θ and φ are the spin directions in the sublattices

direction at various values of the single-ion anisotropy. In this section we shall analyze the phase diagram.

Consider first the ferromagnetic phase, (F), in which the spins are mutually parallel. This phase is described by equations (4)–(6). Note that when the field forms an angle $\gamma = \pi/4$ to the anisotropy axis the equations are easily soluble and the result is

$$\cos\alpha = 0, \quad \sin 2\beta = h(\sqrt{2A^2+h^2}-h)/A^2, \tag{11}$$

where $A = (X-Z+2a)$, $h = \sqrt{h_x^2+h_z^2}$. The energy corresponding to these solutions is the following:

$$X+a-A\sin\beta[\sin\beta+2\cos\beta(\cos\beta-\sin\beta)^{-1}]. \tag{12}$$

Thus, conclusions drawn generally for arbitrary field directions can be verified by the correspondence in this particular case.

Let us examine in a general way the stability conditions for phase F. Since $\partial^2 E/\partial\beta\partial\alpha = 0$ for (4)–(6), these conditions reduce to $\partial^2 E/\partial\alpha^2 \geqslant 0$ and thus one can find that the phase is stable outside the ellipse-like curve described by the parametric equations

$$h_x = \cos\beta(2X - B\cos^2\beta), \quad h_z = \sin\beta(2Z + B\sin^2\beta) \tag{13}$$

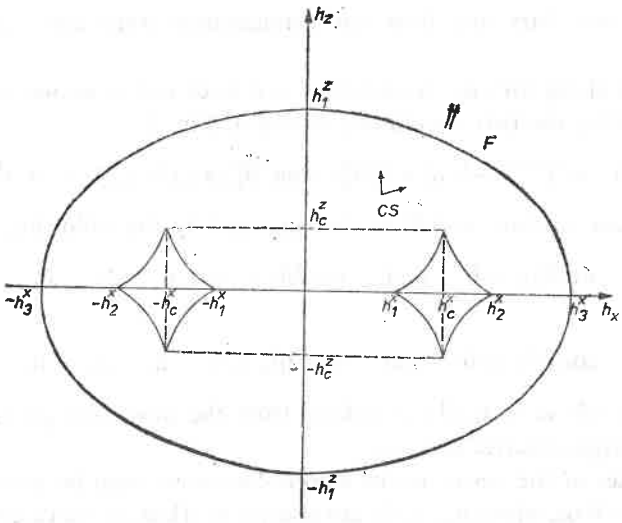

Fig. 2. The schematic phase diagram for $(X-Z) > 2a > 0$. The ellipse-like curve corresponds to Eq. (13), the astroid-like curves to Eq. (18)

and this is illustrated in Fig. 2. It follows from (4) and (13) that at the stability boundary the spin configuration is given by

$$\cos\alpha = 0, \quad \cos 2\beta = \frac{-4a(X+Z) - \{A^2(X+Z)^2 + \frac{1}{4}[A^2 - 16a^2(A^2-4h^2)]\}^{1/2}}{\frac{1}{2}[16a^2 - A^2]}, \tag{14}$$

where A and h are defined by (11).

If the anisotropy constants are appropriately chosen, then the stability boundary corresponds to those derived previously [7, 8], whereas there is no correspondence between (13) and its counterpart given by Eq. (1.9) in [9].

The eventual canted-spin (CS) phases are described by equations (5–6). In this case the condition $\Delta \geqslant 0$ yields the inequality

$$\frac{(1-\sin^2\alpha)[h_x h_z + 2aB\sin^3 2\beta]}{\sin 2\beta} \geqslant 0. \tag{15}$$

One should notice that the left-hand side of (15) leads to the following spin configurations at the stability boundary:

$$\sin^2 \alpha = 1, \tag{16}$$

$$\sin 2\beta = \sigma = -\left(\frac{h_x h_z}{2aB}\right)^{1/3}. \tag{17}$$

The configuration of (16) corresponds to the same ellipse-like stability boundary as that given by (13), which now becomes the upper bound of a CS phase. Inside this stability boundary we have the CS configuration for which $\sin^2 \alpha < 1$. As seen from (16) we have $\sin^2 \alpha = 1$ at the boundary and thus this configuration approaches continuously that of the F phase.

Equation (17), along with the condition $\Delta = 0$ leads to the second stability boundary which is illustrated by the two astroid-like curves in Fig. 2

$$B[X+Z\pm 2a(1-\sigma^2)^{1/2}]^2 - h_x^2 h_1^z + h_z^2 h_3^x - 4a\sigma^2 B[2a \pm (X+Z)(1-\sigma^2)^{1/2}] = 0. \tag{18}$$

Here, two CS phases coexist, which is characterized by the following properties:

$$\sin 2\beta_1 \geqslant 0 \quad \text{and} \quad \sin 2\beta_2 \leqslant 0 \quad \text{if} \quad 2a \geqslant 0, \tag{19}$$

or

$$\cos 2\beta_1 \geqslant 0 \quad \text{and} \quad \cos 2\beta_2 \leqslant 0 \quad \text{if} \quad 2a \leqslant 0. \tag{20}$$

The validity of the above inequalities follows from the inequality given in (15) and the properties of the trigonometric functions.

The coordinates of the cusps on the astroid-like curves can be found by sloving the equations $dh_x/dh_z = 0$ or, where h_x and h_z are given (18). Thus, in the case when $dh_x/dh_z = 0$ we have

$$\cos \beta = 0, \quad \sin \alpha = 0, \tag{21}$$

which corresponds to the coordinates

$$h_z = 0, \quad h_x = \pm h_1^x, \tag{21a}$$

and the second solution,

$$\sin \beta = 0, \quad \sin \alpha = \frac{h_2^x}{h_3^x}, \tag{22}$$

with the cusps at

$$h_z = 0, \quad h_x = \pm h_2^x, \tag{22a}$$

Moreover, the condition $dh_x/dh_z = \infty$ yields the solution

$$\sin 2\beta = \sigma = \pm 1, \quad \sin \alpha = \pm \frac{1}{\sqrt{2}} \sqrt{\frac{B}{h_3^x}}, \tag{23}$$

and the coordinates of the cusps $h_z = h_c^z = \pm 2a \sqrt{\frac{B}{h_3^x}}$, $h_x = h_c^x = \sqrt{B h_3^x}$.

As seen from formulae (21) and (22) and Table I, the solutions obtained and the critical field are the same as those corresponding to the transition from phase AF to CS and from SF to CS. This is an obvious result if one takes into account that $h_z = 0$ corresponds to the field parallel to the easy axis ($h_z = 0$, $h_x = 0$).

The area inside the astroid-like curves can correspond to various spin configurations depending on the sign of $2a = L_z - L_x$ (see Eqs (19), (20)). Thus, if $L_z > L_x$ then the two configurations: $\sin 2\beta_1 \geqslant 0$ and $\sin 2\beta_2 \leqslant 0$ can coexist inside this area. The energies corresponding to these configurations are equal on the straight line $h_z = 0$. This can be found easily if one notes that $\sin 2\beta_1 = \sin 2\beta_2 (\beta_2 = \pi - \beta_1)$ and inserts this to (2). Of course, one can also find the exact solutions for β_1 and β_2 on this line. These are given in Table I for the CS phase.

In the opposite case, i.e., if $L_z < L_x (2a < 0)$, inside the astroid-like curves, we have the configurations for which $\cos 2\beta_1 \geqslant 0$ and $\cos 2\beta_2 \leqslant 0$. The curves on which the energies of both these CS phases are equal are the straight lines $h_z = \pm h_c^z$. This can be found by the following argument. One can assume that on the equal-energy curves the spin configurations of the coexisting phases have the property $\cos 2\beta_1 = -\cos 2\beta_2$, i.e., the same is found when the energies of the AF and SF phases are equal at points $h_x = \pm h_c^x$, $h_z = 0$ of the phase diagram. One can, in turn, determine the general spin configuration

$$\sin 2\beta_1 = \sin 2\beta_2 = -\frac{h_x h_z}{2aB}, \qquad -\cos 2\beta_1 = \cos 2\beta_2, \tag{24}$$

which corresponds to the equal-energy curves. By inserting (24) into (2) we obtain the lines $h_z = \pm h_c^z$ on which the energies of both the CS phases, CS_1 and CS_2, are equal

$$E_{CS_1} = E_{CS_2} = -X + a + a(h_3^x)^2 \sin^2 2\beta/(h_c^x)^2. \tag{25}$$

Finally, if $L_z = L_x (2a = 0)$, we have $h_1^x = \pm h_c^x = \pm h_2^x$, $h_z = 0$ which means that the equation is satisfied by the two points at which the first order phase transition from the AF phase to SF occur.

3. Magnetization and magnetic susceptibility tensor

In this section we shall examine the character of the phase transitions on the stabilities boundaries. To accomplish this we shall examine the behaviour of the magnetization components

$$m^{\parallel} = -\tfrac{1}{2}\frac{\partial E}{\partial h} = \sin\alpha \sin(\gamma + \beta), \tag{26}$$

$$m^{\perp} = -\frac{1}{2h}\frac{\partial E}{\partial \gamma} = \sin\alpha \cos(\gamma + \beta), \tag{27}$$

and the components of the susceptibility tensor

$$\chi^{\parallel} = \frac{\partial m^{\parallel}}{\partial h}, \tag{28}$$

$$\chi_{\perp}^{\parallel} = \chi_{\parallel}^{\perp} = \frac{1}{h}\frac{\partial m^{\parallel}}{\partial \gamma} = \frac{\partial m^{\perp}}{\partial h}, \tag{29}$$

$$\chi_{\perp}^{\perp} = \frac{1}{h}\frac{\partial m^{\perp}}{\partial \gamma}, \tag{30}$$

where $h = \sqrt{h_x^2+h_z^2}$, $h_x = h\sin\gamma$, $h_z = h\cos\gamma$.

TABLE II

The magnetization components when the external magnetic field is parallel or perpendicular to the easy direction and $2a > 0$

$\gamma = \frac{\pi}{2}$	$h_z = 0$	
	$m^{\parallel}$	$m_{\perp}$
AF	0	0
CS	$\frac{(h_x - h_1^x)}{4a}$	$\pm\left\{\frac{1}{4a}\sqrt{\frac{B}{h_1^z}}(h_x-h_1^x)\left[1-\frac{(h_x-h_1^x)^2 h_1^z}{4aB}\right]\right\}^{1/2}$
SF	h_x/h_3^x	0
P	1	0
$\gamma = 0$	$h_x = 0$	
SF	h_z/h_1^z	0
P	1	0

The magnetization and susceptibility components corresponding to $h_z = 0$ or $h_x = 0$ are given in Tables II and III, (see also Table I for the stability regions and Eq. (7)–(9) for the definitions of the critical fields). These results are illustrated in Figs 3–6. One can see that if $2a \geqslant 0$, then all the phase transitions are of the second order except for the case $2a = 0$ when at the point $h_z = 0$, $h_x = \pm h_c^x$ the single point corresponding to the stability boundary (18) the system undergoes the first order phase transition. In the opposite case, when $2a < 0$, the first order phase transition can occur inside the region determined by the stability boundary (18). If this phase transition occurs on the equal-energy straight lines $h_x = \pm k_c^x$, then the jump in the magnetization is the following:

$$m_1^{\parallel} - m_2^{\parallel} = \Delta m^{\parallel} = h_c^x \cos 2\beta_1 [(h_3^x)^2 + 4a^2 \sin^2 2\beta_1]^{-1/2}, \tag{29}$$

$$m_1^{\perp} - m_2^{\perp} = \Delta m^{\perp} = \Delta m^{\parallel} \frac{h_c^z}{h_c^x} \sin 2\beta_1. \tag{30}$$

TABLE III

The susceptibility components when the external magnetic field is parallel or perpendicular to the easy axis and $2a > 0$

$\gamma = \frac{\pi}{2}$	$h_z = 0$		
	$\chi_{\parallel}^{\parallel}$	$\chi_{\parallel}^{\perp}$	$\chi_{\perp}^{\perp}$
AF	0	0	$\frac{X-Z-2a}{(h_1^x)^2-h_x^2}$
CS	$\frac{1}{4a}$	$\frac{h_x^2 \sin^2 2\beta - h_x h_1^x - 2(h_x-h_1^x)^2 \sin^2\beta}{4ah_x h_1^x \sin 2\beta}$	$\frac{h_x^2+h_1^x(h_1^x-2h_x)\sin^2 2\beta}{4ah_x h_1^x \sin^2 2\beta}$
SF	$\frac{1}{h_3^x}$	0	$\frac{(h_c^x)^2 h_3^x + 4ah_x^2}{h_3^x[h_1^z h_x^2 - h_3^x (h_c^x)^2]}$
P	0	0	$\frac{X-Z+2a}{h_x(h_x-X+Z-2a)}$
$\gamma = 0$	$h_x = 0$		
SF	$\frac{1}{h_1^z}$	0	$\frac{(h_1^x)^2 h_1^z - 4ah_z^2}{h_1^z[h_3^x h_x^2 + (h_1^x)^2 h_1^z]}$
P	0	0	$\frac{X-Z+2a}{h_z(h_z+X-Z+2a)}$

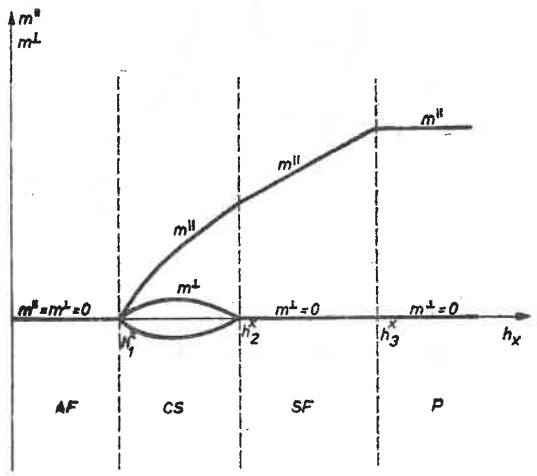

Fig. 3. The schematic dependence of the magnetization components on the field strength when the external magnetic field is parallel to the easy axis ($h_z = 0$) and $L_x < L_z$

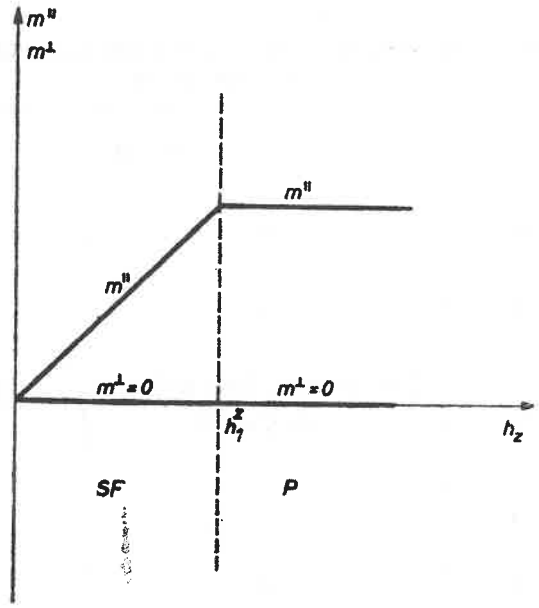

Fig. 4. The schematic dependence of the magnetization components on the field strength when the external magnetic field is perpendicular to the easy axis ($h_x = 0$)

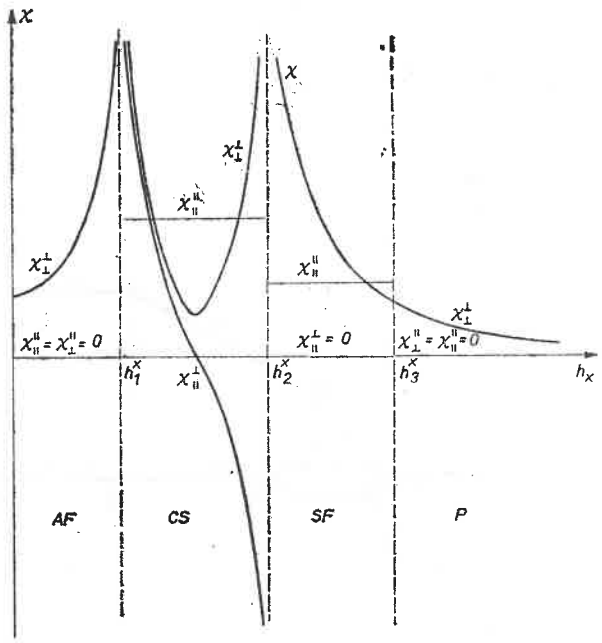

Fig. 5. The schematic dependence of the susceptibility components on the field strength when the external magnetic field is parallel to the easy axis and $L_x < L_z$

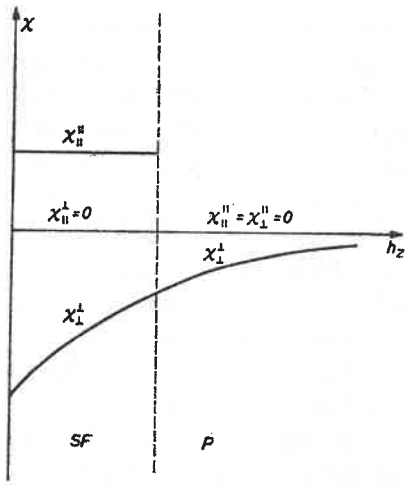

Fig. 6. The schematic dependence of susceptibility components on the field strength when the external magnetic field is perpendicular to the easy axis

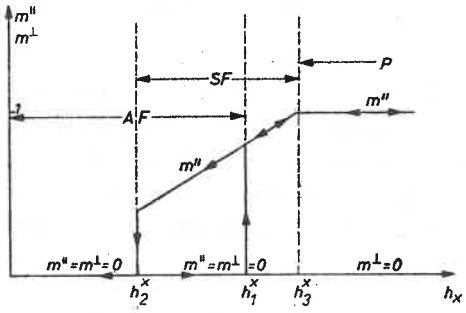

Fig. 7. The schematic dependence of the magnetization components on the field strength when the field is parallel to the easy axis and $L_z < L_x$

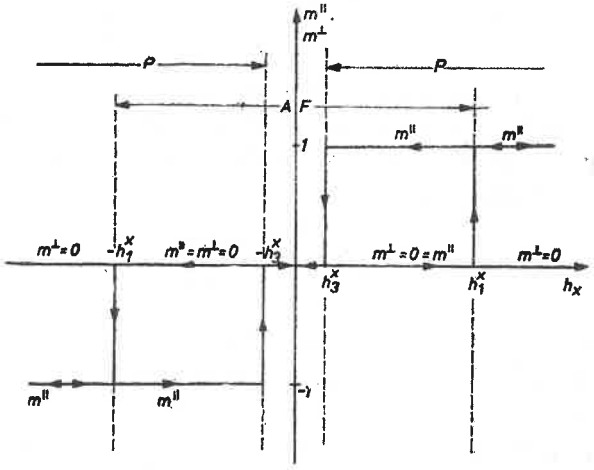

Fig. 8. The dependence of the magnetization components on the field strength when the field is parallel to the easy axis and $2a < -Z$

This corresponds to the transition from the configuration corresponding to $\cos 2\beta_1 \geqslant 0$ to that corresponding to $\cos 2\beta_2 \leqslant 0$ (see, Eq. (20)). The jump in the component m is shown in Fig. 7, which illustrates the dependence of $m^{\parallel}$ and $m^{\perp}$, on h_x.

As seen from Eqs. (29) and (30) $\Delta m^{\parallel} = \Delta m^{\perp} = 0$ if $\beta_1 = \beta_2 = \pm\pi/4$. This correspond to points $h_z = \pm h_c^z$, $h_x = \pm h_c^x$ of the phase diagram. At these points the components of the susceptibility tensor are divergent. This means that these are isolated points of the second-order phase transition or terminal points of the curves of the first order phase transition. It should be noted that if $2a > 0$, i.e., in the opposite case as considered above, these are the points $h_x = \pm h_1^x$, $h_2 = 0$ and $h_x = \pm h_2^x$, $h_2 = 0$ which are isolated points of the second order phase transition, whereas the points $h_2 = \pm h_c^2$, $h_x = \pm h_c^x$ correspond solely to stability boundaries of certain phases such as ($\sin 2\beta_1 \geqslant 0$, $\sin 2\beta_2 \leqslant 0$).

If $2a = L_z - L_x < 0$ and the value of L_x increases, then a direct transition from the AF phase to the P phase can occur. This is obvious from the equations (7)–(9) and Table I. Such a transition is illustrated in Fig. 8 one the $m^{\parallel}$ vs h_x diagram.

4. Influence of the single-ion anisotropy on the phase diagram

In the previous section we focused on the sign of the effective single-ion anisotropy $2a = L_z - L_x$ which can influence the kind of the phase transition. To examine this in the fullest detail we shall first consider how the stability boundaries are changed under the influence of the value of $2a$. For this purpose we will examine the derivative dh_x/dh_z on the stability boundary (13). This derivative is equal to zero at the points $h_z = 0$, $h_x = \pm h_3^x$, regardless of the value of $2a$, and additionally at the points

$$h_4^x = \pm\tfrac{4}{3} X \sqrt{\frac{2X}{3B}}, \tag{31}$$

$$h_4^z = \pm \frac{X+3Z-6a}{3}\left[\frac{X-3Z-6a}{3B}\right]^{1/2}, \tag{32}$$

when $2a \leqslant -Z+X/3$. The stability boundary (13) and its characteristic points in the latter case are shown in Fig. 10. The coordinates of the characteristic points cusps of the second stability boundary (18) are given by (21–23). Taking this into account we can show that if the inequality is satisfied then

$$0 \geqslant 2a \geqslant -\frac{Z(X+Z)}{2X+Z} \tag{33}$$

and the stability boundary (18) is contained within the boundary of (13) as shown in Fig. 9.

If the single-ion anisotropy in the easy direction is strong enough, i.e., if $2a$ is sufficiently small, the curves of the stability boundary intersect. This means that there exists an area in the (h_x, h_z) -plane where the three phases CS_1, CS_2 and F coexist. This area corresponds to the shaded region in Fig. 10. At these points of the curve (18) which are included inside the astroid-like curve (13) the system undergoes the second order phase

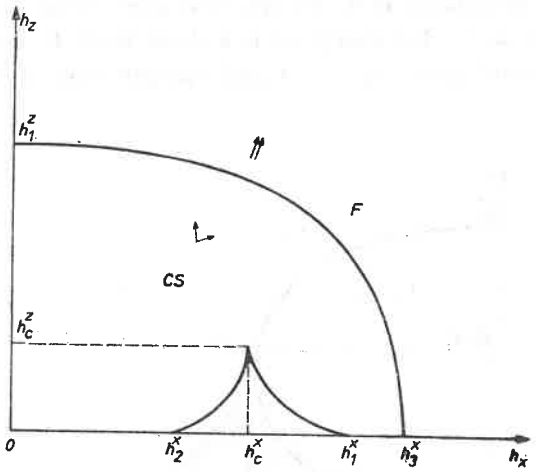

Fig. 9. The phase diagram for $a \geqslant 2a \geqslant \dfrac{-Z(X+Z)}{2X+Z}$

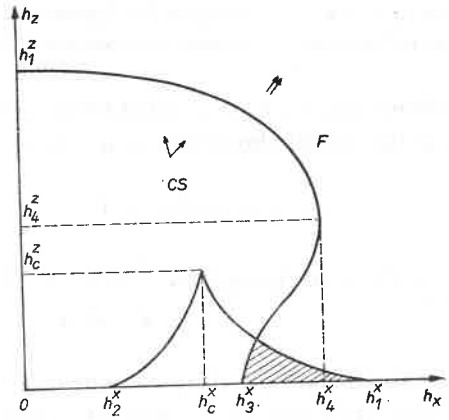

Fig. 10. The phase diagram for $-Z < 2a < -Z \cdot (X+Z)/2X+Z$

transition between the CS and F phases because $\sin^2 \alpha = 1$ in the F and CS, the phases and the magnetization is continuous through the transition.

If $2a$ decreases so much that its value reaches $-Z$, then the stability boundary (13) is tangent to the straight line $h_x = \pm h_c^x$ and at the point of tangency the energies of the F and CS_2 phase are equal. This results from the fact that the energies of both the CS phases are equal on the line $h_x = \pm h_c^x$ and, on the other hand, the energies of the F ans CS, phase are equal on the stability boundary (13).

With a further decrease of $2a$, if its value is equal to $-Z-X/3$, the curve (13) is tangent to the straight lines $h_x = \pm h_c^x$ and also to curve (18) at some of the cusps Fig. 11, there this is illustrated for $h_x > 0$, $h_z > 0$. As can be seen from Fig. 11, there is another tangent point of the stability boundaries (13) and (18) which is marked by C. In the shaded area

between the stability boundaries (13) and (18) first order phase transitions between the phases CS_2 and F can occur. The exception is a single point $h_z = h_c^z$, $h_x = h_c^x$, at which $\cos\alpha_F = \cos\alpha_{CS_2} = 0$ and $\beta_F = \beta_{CS_2} = \pi/4$ and the transition is of the second order.

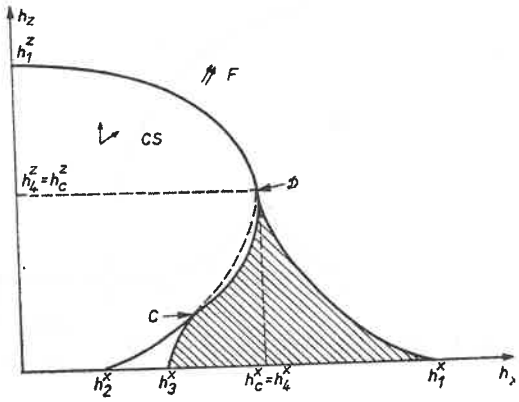

Fig. 11. The phase diagram for $2a = -Z - X/3$. The dash line denotes that the condition $\sin^2\alpha \leqslant 1$ is not satisfied. In the shaded region first order phase transitions between the phases CS_2 and F can occur

This is clearly seen if the above equalities are inserted to the formulae (26) and (27). Generally, the tangency points of the stability boundaries correspond to the spin configurations:

$$\cos\alpha_F = \cos\alpha_{CS} = 1, \tag{34}$$

$$\cos 2\beta_{CS} = \cos 2\beta_F = \frac{2(X+Z) \pm \sqrt{B^{-1}[64a(X+Z)^2 - (X-Z-18a)(X-Z-6a)^2]}}{(X-Z-18a)}, \tag{35}$$

where the upper sign refers to point D and the lower one to point C in Fig. 11.

With further decrease of $2a$ toward $2a = -(X+Z)$, point C approaches the origin of the coordinate frame. The phase diagram for $2a = -(X+Z)$ is shown in Fig. 12. Below this value of $2a$ there exists an area in the phase diagram where two F phases metastable with respect to CS can occur (shaded area of Fig. 13).

Regardless of the fact that equations (4)–(6) are not analytically soluble for an arbitrary field direction, one can draw some conclusions concerning the behaviour of $m^{\parallel}$ and $m^{\perp}$ under the change of $2a$. For this purpose we write the formulae for $m^{\parallel}$ and $m^{\perp}$ in the following way:

$$m^{\parallel} = \frac{(X+Z+2a\cos 2\beta)\sin^2\alpha}{h}, \tag{36}$$

$$m^{\perp} = -\frac{(X-Z-2a\cos 2\alpha)\sin 2\beta}{2h}. \tag{37}$$

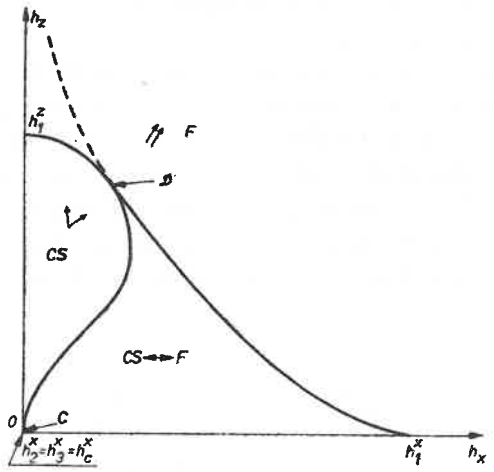

Fig. 12. The phase diagram for $2a = -(X+Z)$. The dash line denotes that the conditions $\sin^2\alpha \leqslant 1$ is not satisfied

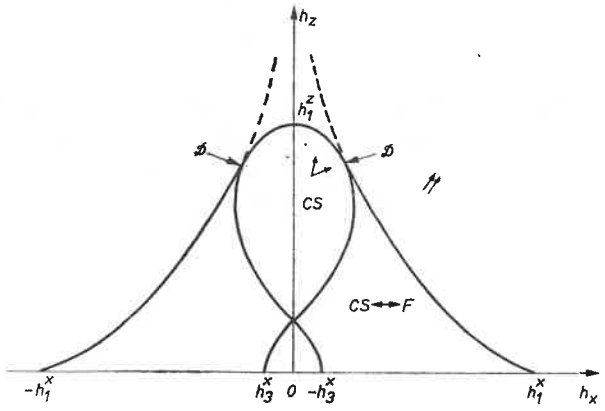

Fig. 13. The phase diagram for $2a < -(X+Z)$

Here we took advantage of equations (4)–(6). It can be seen that $m^{\parallel} \geqslant 0$ regardless of the values of h and $2a$, whereas the sign of $m^{\perp}$ depends on the spin configuration and can be changed under the influence of the field. If the system is in the F phase, when $\cos\alpha = 0$, we have:

$$m^{\perp} = -\frac{(X-Z+2a)\sin 2\beta}{2h}. \tag{38}$$

Thus, in this case $m^{\perp} < 0$ if $2a > -(X-Z)$ and $m^{\perp} > 0$ if $2a < -(X-Z)$. If $2a = -(X-Z)$ then the perpendicular magnetization is equal to zero and is independent of the strength of the field. If $2a < -(X-Z)$, we can also conclude that the spin direction

is between that of the field and the effective hard axis if $2a > -(X-Z)$ and between that of the field and the effective easy axis.

It is also possible to find the spin configuration in the CS phase if $2a < -(X-Z)$. Since the second order phase transitions occur and $m^{\perp} > 0$ on the stability boundary (13), $m^{\perp}$ vanishes for some values of the field components in the region of the CS phase. This means that for these values of field components the spins of the two different sublattices form the angles $\pm\xi$, of the same magnitude but different sign to the direction of the field. Bearing this in mind and taking into account the equations (5)–(6) we now find that $m^{\perp} = 0$ for h and γ (for definition of h and γ see Fig. 1) satisfying the equation:

$$\cos^2\gamma = \frac{h - h_3^x\sqrt{-\frac{B}{4a}}}{4a\sqrt{-\frac{B}{4a}}}, \tag{39}$$

which corresponds to the angle ξ given by

$$\cos^2\xi = -\frac{B}{4a}. \tag{40}$$

It can be seen that the angle ξ is independent of the magnitude and direction of the external field but this solely depends on the material constants.

One can also note that Eq. (39) and (40) have a physical sense if $2a \leqslant -(X-Z)$, i.e., that is, equation $m^{\perp} = 0$ have physical solutions if this condition is satisfied.

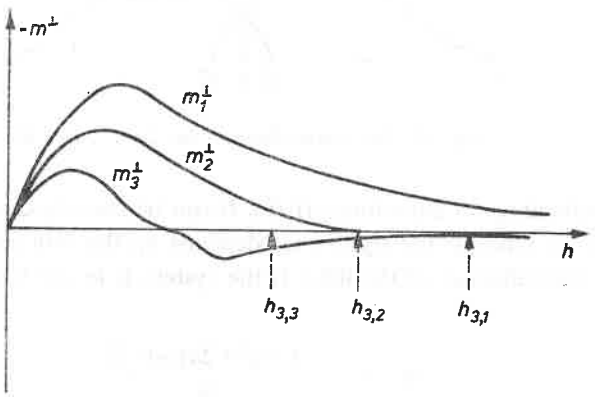

Fig. 14. The schematic dependence of the perpendicular magnetization components on the field strength when the angle γ of the field is such that $\mathrm{tg}\gamma < |h_c^z/h_c^x|$ $m_1^{\perp}$ corresponds to $2a > -(X-Z)$, $m_2^{\perp}$ to $2a = -(X-Z)$, $m_3^{\perp}$ to $2a < -(X-Z)$. Note that the existence of an inflection point at $m^{\perp} = 0$, which follows from the vanishing of $\chi_{11}^{\perp}$

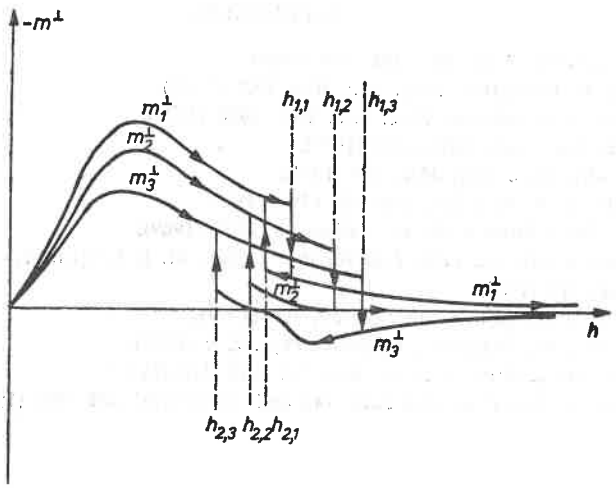

Fig. 15. The schematic dependence of the perpendicular magnetization on the field strength when γ satisfies $\mathrm{tg}\,\gamma > |h_c^z/h_c^x|$, $m_1^{\perp}$ corresponds to $2a > -(X-Z)$, $m_2^{\perp}$ to $2a = -(X-Z)$, $m_3^{\perp}$ to $2a < -(X-Z)$. $h_{2,1}$, $h_{2,2}$, $h_{2,3}$, $h_{1,1}$, $h_{1,2}$, $h_{1,3}$ denote the stability boundary (18) for the assumed value of γ

The above discussion together with equations (29) and (30) allow us to draw a schematic dependence $m^{\perp}$ on h. Fig. 14 shows this dependence for such a direction of the field that $\mathrm{ctg}\,\gamma > h_c^z/h_c^x$ and Fig. 15 this dependence if $\mathrm{ctg}\,\gamma < h_c^z/h_c^x$.

5. *Concluding remarks*

The results of this paper are valid, in principle, for the values of the single-ion anisotropy which are comparable with the exchange integral. However, we should also realise that our approximate ground state coresponds to a classical expression if the value of S is sufficiently large. In this case our results should be also valid for large values of the single-ion anisotropy. Such an approximation seems to be justified if the external magnetic field applied parallelly to the easy axis, for the energy of the zero-point motion, is then negligible. Thus, our results should be approximately valid also for the metamagnetic case.

It is note worthy that our results correspond to those of others [5–8], except for some of the results reported in [8]. These concern the order of the transition at the cusp of the astroid-like stability boundary. As seen from our report this is the second-order phase transition that the system undergoes at the cusp, whereas according to [8] there occurs a first order phase transition. The second discrepancy concerns the susceptibility tensor which, as seen from our studies, should be symmetric at each point of the phase diagram. Due to the approximations made in [8] this symmetry has been broken.

There are also some disagreements with the results presented in [9] for the metamagnetic case. This is due to the discrepancy in the stability boundaries which has been erroneously derived in [9]. In particular, this concerns Eq. (1.9) of [9] that, as can be shown, does not satisfy the condition for a minimum of the free energy. This propably leads to different regions of metastability than those obtained in this paper.

REFERENCES

[1] J. Feder, E. Pytte, *Phys. Rev.* **168**, 640 (1968).
[2] J. E. Rives, V. Benedict, *Phys. Rev.* **B12**, 1908 (1975).
[3] J. E. Rives, S. N. Bhatia, *Phys. Rev.* **B12**, 1920 (1975).
[4] M. Cieplak, *Phys. Rev.* **B15**, 5310 (1977).
[5] G. Kozłowski, *Phys. Lett.* **35A**, 359 (1971).
[6] M. Yamashita, *J. Phys. Soc. Jap.* **32**, 610 (1972).
[7] M. Rohrer, M. Thomas, *J. Appl. Phys.* **40**, 1025 (1969).
[8] C. K. Chepurnykh, *Fiz. Tver. Tela* **10**, 1917 (1968). M. J. Kaganov, C. K. Chepurnykh, *Fiz. Tver. Tela* **11**, 911 (1969).
[9] A. J. Mitzek, *Phys. Status Solidi* (b) **59**, 309 (1973).
[10] G. Kozłowski, W. Prystasz, *Commun. Phys.* **2**, 9 (1977).
[11] M. Pfeiffer, W. J. Ziętek, *Acta Phys. Pol.* **A38**, 176 (1970).
[12] G. Kozłowski, *Acta Phys. Pol.* **A47**, 183 and 493 (1975); **A48**, 201 (1975).